

Influence of dipole interaction on lattice dynamics of crystalline ice

W.A. ADEAGBO* and P. ENTEL

Institute of Physics,

University of Duisburg-Essen, Duisburg Campus, 47048 Duisburg, Germany

(Received November 16, 2017)

Abstract

The Born effective charges of component atoms and phonon spectra of a tetrahedrally coordinated crystalline ice are calculated from the first principles method based on density functional theory within the generalized gradient approximation with the projected augmented wave method. Phonon dispersion relations in a $3 \times 1 \times 1$ supercell were evaluated from Hellmann-Feynman forces with the direct method. This calculation is an additional work to the direct method in calculating the phonon spectra which does not take into account the polarization charges arising from dipole interaction of molecules of water in ice. The calculated Born effective polarization charges from linear response theory are supplied as the correction terms to the dynamical matrix in order to further investigate the LO-TO splitting of the polar modes of ice crystal at $\mathbf{k} = 0$ which has long been speculated for this system especially in the region between 28 and 37 meV both in the theoretical and experimental studies. Our results clearly show the evidence of splitting of longitudinal and transverse optic modes at the $\mathbf{k} = 0$ -point in agreement with some experimental findings.

Keywords: Ice, Density functional calculations, Phonon spectra, Born effective charges

1. INTRODUCTION

The vibrational studies of solid ice have gained attraction for scientific investigation over the decades. Experimentally, the vibrational spectra of the

*Corresponding author. Tel. +49 203 379 1606; fax: +49 203 379 3665.
E-mail: adeagbo@thp.uni-duisburg.de

different phases of ice have been investigated using infra-red (IR) and Raman techniques, but due to the proton disordering in most such structures, the normal selection rules governing the interaction of radiation with these lattices are broken and hence any analysis of the spectra is difficult. On the other hand, the IR and Raman spectra are very sensitive to the intramolecular modes involving O-H stretching and bending, and less sensitive to the intermolecular modes involving the vibrations where the whole water molecules are moving against each other. Therefore, in normal circumstances, only limited information (the acoustic frequencies in particular) can be obtained in the translational region. Inelastic incoherent neutron scattering (IINS) is only more reliable because its spectrum is directly proportional to the phonon density of states weighed by mean square amplitude associated with each mode and also the selection rule is not involved as all modes are measured simultaneously [1, 2]. Despite the detail information that can be obtained from the present days methods of coherent and incoherent scattering on the vibrational motions of the atoms or molecules of most systems based on the peak positions, intensities and their width, there are still many problems about the ice systems. These problems as mentioned, are usually associated with the the proton disordering. The phonon spectra measurements of Renker [3] on Ice-Ih (D_2O) made by time of flight using a chopper spectrometer were extensive but not complete in that information above 20 meV in the (001) direction and above 30 meV in other directions is missing, presumably because of a lack of scattering intensity and of the nature of the disordering of the protons in the ice structure.

First-principles calculation of crystal structure and crystal properties is becoming standard technique, and the progress in the methods, algorithms, and computer capabilities allows to study larger systems of solids crystals in which crystalline ice cannot be left out. The method has recently gained ground not only because of its reliability in the study of static and dynamics properties of ice [4, 5] but also some important features such as modeling ordered periodic ice structure [6], and also to probe the nature of hydrogen bond in different geometries [7]. Its theoretical counterpart such as the classical modeled potential through empirical method [8, 9] had some success in describing some important dynamical features, but to date, there is none capable of describing the ice dynamics and related properties across its whole spectral range and describing certain key spectral features.

There are two techniques currently in use in the first-principles method in the study of lattice dynamics of crystals: The linear response method and the direct method. In the linear response method the dynamical matrix is obtained from the modification of the electron density, via the inverse dielectric matrix. The dielectric matrix is calculated from the eigenfunctions and energy levels of the unperturbed system [10]. It can be determined at any wave vector in the Brillouin zone with the computational effort required comparable to that of a ground state optimization. Only linear effects, such as harmonic phonons, are accessible to this technique. On the other hand,

the direct-method is based on the solution of the Kohn-Sham equation and it allows one to study both linear and non-linear effects. The calculations deal with a supercell, which allows explicit account to be taken of any perturbation. This method is rather straightforward computationally and there are a few standard software packages. Within the direct method the phonon frequencies are calculated from Hellmann-Feyman forces generated by the small atomic displacements, one at a time. Hence using the information of the crystal symmetry space group the force constants are derived, and the dynamical matrix is built and diagonalized, and its eigenvalues arranged into phonon dispersion relations. In this way, phonon frequencies at selected high frequencies at high-symmetry points of the Brillouin zone can be calculated [11]. However, when the interaction range ceases to be within the supercell, phonons at all wave vectors are determined exactly. The above statement has to be modified for polar crystals for which the macroscopic electric field splits off the infrared-active optic modes. The long-range part of the Coulomb interaction corresponds to the macroscopic electric field arising from ionic displacements.

Ice is a tetrahedrally covalently bonded polar system whose dipole-dipole interactions give rise to the electric field when they are disturbed. The origin of the splitting is therefore the electrostatic field created by long wavelength modes of vibrations in such crystals. Usually a microscopic electric field influences only the LO modes while TO modes remain unaltered. The field therefore breaks the Born-von Kármán conditions, as a consequence with a direct method only finite wave vector $\mathbf{k} \neq 0$ calculations are possible. The LO/TO splitting has therefore been found by calculating the effective Born charge tensor and electronic dielectric constant introduced into the dynamical matrix in the form of a non-analytical term [12] or by calculating LO modes from elongated supercells [13] as will be discussed below.

In our previous work, we have applied with success the direct method to the calculation of phonon dispersion of ice and its corresponding vibrational density of states [14]. The method reproduces the important features in the translational mode, librational mode, bending as well as the stretching region in comparison to the experimental results. The only ingredient that was missing in the previous work has been explained above, i.e., a macroscopic electric field arising from dipolar interaction which is not taken into account. Despite the huge computational demand of this problem, we did the additional calculation of Born-effective charges which is supplied as ingredients to the direct method to identify the long-range part of interatomic force constants and makes the interpolation of phonon frequencies tractable. Our overall aim is to help resolve the discrepancies in the reported phonon frequencies especially the puzzle behind the LO/TO splitting of some optical modes at $\mathbf{k} = 0$ and provide first principles Born-effective charges and dielectric tensors for direct method phonon calculations.

2. METHOD OF CALCULATION

The calculation of phonon dispersion relations were performed with the direct method. The direct method uses the Hellmann-Feymann (HF) forces calculated for the optimized supercell with one atom displaced from equilibrium position, derived from the force constants using the symmetry elements of the space group of the crystal, and calculates phonon frequencies by diagonalizing the dynamical matrix.

In this work, the ice crystal structure optimization and calculation of HF forces have been performed with the density functional theory using the PAW method within the generalized gradient approximation (GGA), as implemented in the Vienna *Ab Initio* Simulation Package (VASP) [15] software. A unit cell of ice crystal was prepared in a cubic box according to Fig. 1 with 8 molecules of water. All the atomic degrees of freedom were relaxed with high precision. The optimum Monkhorst Pack of $4 \times 4 \times 4$ k -point was used in addition to the GGA of Perdew-Wang to describe the exchange-correlation and the hydrogen bonding of water. We used a energy cut-off of 500 eV because the 2p valence electrons in oxygen require a large plane wave basis set to span the high energy states described by the wavefunction close to the oxygen nucleus, and also the hydrogen atoms require a larger number of planes waves in order to describe localization of their charges in real space. The relaxed geometry for the unit cell from the initial configurations containing 8 molecules is shown in Fig. 1. The starting geometry of the molecules in the cubic simulation box shown is such that no hydrogen bonds were present but the positions of oxygen atoms follow the tetrahedral geometry. After the relaxation, all the protons perfectly point to the right direction of oxygen atoms and make the required hydrogen bonds necessary as indicated by the dotted lines in Fig. 1 to preserve the tetrahedral orientation of the ice structure. This final structure is in accordance to Bernal Fowler's rules [16] which are based on the statistical model of ice.

The relaxed geometry is tetragonal with calculated lattice parameters $a = 6.1568 \text{ \AA}$, $b = 6.1565 \text{ \AA}$, $c = 6.0816 \text{ \AA}$ i.e. with c/a ratio ≈ 0.988 . The experimental lattice constant reported by Blackman *et. al.* [17] is 6.35012652 \AA for the cubic geometry. The calculations of force constants was carried out by considering a $3 \times 1 \times 1$ supercell containing 24 molecules of water which is obtained by matching 3 tetragonal unit cells. At the first step of the calculation, the PHONON software is used to define the appropriate crystal supercell for use of the direct method. The phonon frequencies $\omega(\mathbf{k}, j)$ are calculated as square roots of eigenvalues of the supercell dynamical matrix:

$$\mathbf{D}^{\text{SC}}(\mathbf{k})e(\mathbf{k}, j) = \omega^2(\mathbf{k}, j)e(\mathbf{k}, j), \quad (1)$$

where the $e(\mathbf{k}, j)$ are the polarization vectors. The supercell dynamical matrix is defined as

$$\mathbf{D}^{\text{SC}}(\mathbf{k}, \mu\nu) = \frac{1}{\sqrt{M_\mu M_\nu}} \sum_{m \in SC} \Phi^{\text{SC}}(0, \mu; m, \nu) \quad (2)$$

$$\times \exp(-2\pi i \mathbf{k} \cdot [\mathbf{R}(0, \mu) - \mathbf{R}(m, \nu)]),$$

where the summation over m runs over all atoms of the supercell; M_μ , M_ν and $\mathbf{R}(0, \mu)$, $\mathbf{R}(m, \nu)$ are atomic masses and equilibrium vectors, respectively; and \mathbf{k} is the wavevector. The cumulant force constants Φ_{ij}^{SC} are the sums of terms containing the second derivatives of the ground-state energy with respect to the position vectors of interacting atoms i and j . The HF forces in the direct method are derived using

$$\mathbf{F}_i(n, \nu) = - \sum_{m, \nu, j} \Phi_{ij}^{\text{SC}}(n, \nu; m, \mu) \mathbf{u}_j(m, \mu), \quad (3)$$

where $\mathbf{u}_j(m, \mu)$ is an amplitude of displacement of an atom in the supercell specially shifted from the equilibrium position.

The symmetry of the supercell and the site symmetry of the non-equivalent atoms usually considerably reduce the number of displacements needed for reconstruction of Φ_{ij}^{SC} . We are unfortunate in our case because of the hydrogen bonding fluctuations which makes the crystal structure complicated. Therefore, we have to consider the whole 24 atoms in the supercell as independent displacements: In the positive and negative non-coplanar, x , y and z directions. As done for the primitive unit cell, all the internal coordinates were relaxed until the atomic forces were less than 10^{-4} eV/Å. Complete information of the values of force constants were obtained by displacing every atom of the primitive unit cells by 0.02 Å in both positive and negative x , y and z directions. Therefore, minimization of the anharmonic effects and systematic errors are achieved by calculating Φ_{ij}^{SC} with Eq. 3 using forces arising from both positive and negative displacements \mathbf{u}_j . As mentioned above, we use a $3 \times 1 \times 1$ supercell, which implies that 3 points in the direction [100] are treated exactly according to the direct method. The points are $[\zeta 00]$, with $\zeta = 1, 1/3, 2/3$. We calculate forces induced on all atoms of the supercell when a single atom is displaced from its equilibrium position, to obtain the force constant matrix, and hence the dynamical matrix. This is then followed by diagonalization of the dynamical matrix which leads to a set of eigenvalues for the phonon frequencies and the corresponding normal-mode eigenvectors. The vibrational density of states (VDOS) is obtained by integrating over \mathbf{k} -dependent phonon frequencies from the force-constant matrix in supercells derived from the primitive molecule unit cells.

For the ionic crystals the macroscopic electric field is taken into account by adding to Eq. (1) the non-analytic term of the dynamical matrix at the wave vector $\mathbf{k} = 0$ [18]. However, since one knows the phonon frequencies only at discrete wave vectors, it is justified to extend the non-analytical term to the $\mathbf{k} \neq 0$ region, through multiplying it by the Gaussian damping factor. Therefore we replace Eq. (1) by the following expression:

$$\begin{aligned} \mathbf{D}_{\alpha, \beta}^M(\mathbf{k}; \mu \nu) &= \mathbf{D}_{\alpha, \beta}^{\text{SC}}(\mathbf{k}; \mu \nu) \\ &+ \frac{4\pi e^2}{V \epsilon_\infty \sqrt{M_\mu M_\nu}} \frac{[\mathbf{k} \cdot \mathbf{Z}^*(\mu)]_\alpha [\mathbf{k} \cdot \mathbf{Z}^*(\nu)]_\beta}{|\mathbf{k}|^2} \end{aligned}$$

$$\begin{aligned}
& \times \exp[-2\pi i \mathbf{g} \cdot (\mathbf{r}(\mu) - \mathbf{r}(\nu))] \\
& \times d(\mathbf{q}) \exp \left\{ -\pi^2 \left[\left(\frac{k_x}{\rho_x} \right)^2 + \left(\frac{k_y}{\rho_y} \right)^2 + \left(\frac{k_z}{\rho_z} \right)^2 \right] \right\}, \quad (4)
\end{aligned}$$

where \mathbf{k} is the wave vector within the Brillouin zone with its centre at the reciprocal-lattice vector \mathbf{g} , V stands for the volume of the primitive unit cell, and M_μ , \mathbf{r}_μ are atomic masses and internal positions, respectively. The $\mathbf{Z}^*(\mu)$ are the tensors of the Born-effective charges. ϵ_∞ is the electronic part of the dielectric constant and ρ (x , y and z) are damping factors; then the non-analytical term vanishes close to the zone boundary. Consideration of the effective charges leads to the LO/TO splitting of the optical parts of the phonon modes of ice at the Γ -point as discussed in the next Section. This observation has long been speculated both from theory and experiment. By definition [19], the Born effective charge tensor $\mathbf{Z}^*_{i,\alpha\beta}$ quantifies to linear order the polarization per unit cell (\mathbf{P}) generated by zone-center $\mathbf{k}=0$, created along the direction β when the atoms of sublattice i are displaced in the direction α under the condition of zero electric field. It is calculated according to the equation:

$$\mathbf{Z}^*_{i,\alpha\beta} = \mathbf{Z}_i + \Omega \frac{\partial \mathbf{P}_\alpha}{\partial \mathbf{u}_{i,\beta}}. \quad (5)$$

The macroscopic dielectric constant is found via the relation

$$\epsilon_\infty = 1 + \frac{4\pi \mathbf{P}}{\mathbf{E}}, \quad (6)$$

where $\mathbf{E} = \mathbf{E}_{ext} - 4\pi \mathbf{P}$ is the total macroscopic electric field.

3. RESULTS AND DISCUSSION

Table I shows the dielectric constants of the ϵ_∞ tensor and the Born-effective charges calculated according to Eq. (6) and (5) implemented in PWSCF_{2.1} code [20]. The dielectric constant tensor is symmetric with non-zero off-diagonal terms but with negligibly contribution in comparison to the diagonal element. The diagonal term ~ 1.88 is in a very good range for the high frequency limit (Thz) of the dielectric constant of ice [21]. Under an applied field the individual molecules are polarized by the field. This involves the displacements of the electrons relative to the nuclei and small distortions of the molecules under the restoring forces. The response to a change in field is very rapid, so that the effects are independent of frequency up to microwave frequencies. The polarization in ice in general is due to the reorientation of molecules or bonds, that is, the energies of some of the proton configurations,

that are compatible with the ice rules [16, 22], are lowered relative to others, so that in thermal equilibrium there is net polarization of ice. The achievement of this equilibrium state is a comparatively slow process that requires thermal activation and local violations of the ice rules.

Our results for the dynamical effective charges are shown in Table I for 24 non-equivalent atoms. The complication of the system due to the protons re-orientation and the hydrogen bonding make the symmetry consideration difficult. The charge neutrality condition [18] requires that the acoustic mode frequencies vanish for $\mathbf{k} = 0$ such that

$$\mathbf{Z}_{i,\alpha\beta}^* = 0. \quad (7)$$

Therefore, this condition is satisfied to at least order of 10^{-4} electron which is accurate enough for any reliable calculation. The unequal effective charge tensor components Z_{H}^* and Z_{O}^* of each hydrogen and oxygen atoms $Z_{xx}^* \neq Z_{yy}^* \neq Z_{zz}^*$ are due to the broken symmetry arising from the lattice distortion. The values alternate among the component atoms of H and also for O in order to preserve the overall neutrality. For instance, the Z_{zz}^* of the hydrogen atoms is $0.624(\pm 0.001)$ electron, while the other two elements Z_{yy}^* and Z_{zz}^* alternate within $0.666(\pm 10^{-4})$ electron. The off-diagonal elements have the values which ranges within ± 0.408 , ± 0.407 , ± 0.402 , ± 0.377 and ± 0.382 with deviation $\pm 10^{-4}$ electron. Similar features are observed for the oxygen atoms with $Z_{zz}^* -1.070 \pm 10^{-4}$ electrons while Z_{xx}^* and Z_{yy}^* alternate between -1.084 and -0.961 with deviation $(\pm 10^{-4})$ electrons. Some of the off-diagonal contributions are too small. The observed anisotropic features can be attributed to the complexity of the hydrogen bond during the electron transfer process and also due to the dipole interaction of the water molecules in Eq. 4.

Figure 2 shows the dispersion relation obtained by supplying the calculated effective charges and the corresponding highest frequency dielectric constants, shown in Table I, as the correction from the analytical term which was added to the dynamical matrix as explained in Section 2. We also compare the dispersion obtained in the absence of these charges to see the magnitude of splitting in the optical mode. The calculated VDOS for both dispersions do not appreciably change much because the states are not complete as it requires summation over all points in the first Brillouin zone. The LO modes that was formally degenerate in the absence of Z^* at 27.1 meV in the translational region is now shifted to a higher value 30.2 meV as shown in Fig. 3. Except for the isotopic effect due to the different masses of hydrogen and deuterium atoms in ice (see the experimental dispersion on the right of Fig. 3). This observation correctly shows the splitting in the optical modes due to the dipole interaction of the water molecules which correspondingly induce a dipole moment in the optical mode. Apart from the translational region, as shown in Fig. 4, other splitting of LO modes occur at 111.0 meV in the librational region with a small shift to 112.5 meV. Also, there is a small shift of 0.1 meV from 204.6 meV in the bending region. The large shift of

about 12.0 meV is observed from 362 meV in the stretching region because the strength of dipole interaction is large when there is symmetric stretching (ν_1) of O-H bond, while a tiny effect observed in the antisymmetric stretching is due to the compensation arising from simultaneous bond lengthening and shortening of the O-H covalent bond.

4. SUMMARY

In summary, we have performed the analysis of the lattice dynamics in crystalline tetrahedrally coordinated ice and found a very strong influence of the dipole interaction on the phonon spectra in the optical regions of ice. *Ab initio* calculations clearly show the splitting in the region between 27.1 and 30.2 meV of the translational region. This observation can be correlated with the experimental observation using high resolution inelastic neutron measurements of the phonon density of states, in which two separate molecular optical bands at about 28 and 37 meV for ice Ih and ice Ic have been observed [2]. Other splitting of LO modes in the librational, bending and stretching region were also predicted due to the dipole interactions. The calculation also shows the extent to which the direct method can be used to calculate the phonon spectra of the dipole system. To our knowledge, a strong influence of the dipole interaction on the lattice dynamics of ice from effective charges calculation was not yet reported.

Acknowledgments

We acknowledge the support by the Deutsche Forschungsgemeinschaft (Graduate College 277 “*Structure and Dynamics of Heterogeneous Systems*”).

References

- [1] J.C. Li, D. London, D.K. Ross, J.L. Finney, S.M. Bennington and A.D. Taylor, Inelastic incoherent neutron scattering and study of ice Ih, II, IX, V and VI in the region from 50-500 meV. *J. Phys. Condens. Matter* **4** 2109 (1994).
- [2] J. Li, Inelastic neutron scattering studies of hydrogen bonding in ices. *J. Chem. Phys.* **16** 6733 (1996).
- [3] B. Renker and P.V. Blanckenhagen, *Physics and Chemistry of Ice*, edited by E. Whalley, S.J. Hones and L.W. Gold (University of Toronto Press, Toronto, 1973), p. 82

- [4] A.S. Cote, I. Morrison, X. Cui, S. Jenkins and D.K. Ross, *Ab-initio* density-functional lattice-dynamics studies of ice. *Can. J. Phys.* **81** 115 (2003).
- [5] I. Morrison and S. Jenkins, First-principles lattice dynamics studies of the vibrational spectra of ice. *Physica B* **81** 115 (1999).
- [6] C. Lee and D. Vanderbilt and K. Laarsonen and R. Car and M. Parrinello, *Ab-initio* studies on the structural and dynamical properties of ice. *Phys. Rev. B* **47** 4863 (1993).
- [7] S.S. Xantheas and H.T. Dunning, *Ab initio* studies of cyclic water clusters $(\text{H}_2\text{O})_n$, $n = 1\text{-}6$. I. Optimal structures and vibrational spectra. *J. Chem. Phys.* **99** 8774 (1993).
- [8] M. Marchi and J.S. Tse and M. Klein, Lattice vibrations and infrared absorption on ice Ih. *J. Chem. Phys.* **85** 2414 (1986).
- [9] G. Nielson and R.M. Townsend and S.A. Rice, Model based calculations of the lattice mode spectra of ice Ih and amorphous solid water. *J. Chem. Phys.* **81** 5288 (1984).
- [10] R. Riesta, *Festkörperprobleme: Advances in Solid-State Physics*, Vol. 25, edited by P. Gross (Vieweg, Braunschweig, 1985).
- [11] K. Parlinski, *Phonon Software*, version 4.11 (Parlinski, Cracow, Poland, 2002).
- [12] W. Zhong, R.D. King-Smith and D. Vanderbilt, Giant LO-TO splittings in perovskite ferroelectrics. *Phys. Rev. Lett.* **72** 3618 (1983).
- [13] K. Parlinski, J. Lažewski and Y. Kawazo, *Ab-initio* study of phonons in MgO by the direct method including LO mode. *J. Phys. Chem. Solids* **61** 87 (1999).
- [14] W.A. Adeagbo, A. Zayak and P. Entel, *Ab-initio* study of structure and dynamical properties of crystalline ice. *Phase Transitions* **78** 179 (2005).
- [15] G. Kresse, J. Fethmüller, Efficient iterative schemes for *ab initio* total-energy calculations using a plane-wave basis set. *Phys. Rev. B* **54** 11169 (1996).
- [16] J.D. Bernal and R.H. Fowler, A theory of water and ionic solution. *J. Chem. Phys.* **1** 515 (1933).
- [17] Electron diffraction investigation into cubic and other structural forms of ice *Adv. Phys.* **7** 189 (1958).

- [18] R. Pick, M.H. Cohen and R.M. Martin, Microscopic theory of force constants in the adiabatic approximation. *Phys. Rev. B* **1** (1970).
- [19] R. Yu and H. Krakauer, Linear-response calculations within the linearized augmented plane-wave method. *Phys. Rev. B* **49** 4467 (1994).
- [20] S. Baroni, A. Dal Corso, S. de Gironcoli and P. Giannozzi, *PWSCF and PHONON: Plane-wave pseudo-potential codes*, <http://www.pwscf.org> (2001).
- [21] V.F. Petrenko and R.W. Whitworth, *Physics of Ice*, (Oxford University Press, Oxford, 1999).
- [22] L. Pauling, The structure and entropy of ice and of other crystals with some randomness of atomic arrangement. *J. Am. Chem. Soc.* . **57** 2680 (1935).

TABLES

Table 1 Calculated dielectric constants and Born effective charges of cubic ice using linear response in PWSCF_{2.1} code [20].

FIGURE CAPTIONS

Fig. 1 Initial and the relaxed geometry of the unit cell of ice. The ice structure was initially packed in a cubic unit cell with initial lattice constant taken from the literature [6] to be 6.35 Å. There are no hydrogen bonds in the initial prepared structure shown on the left but were perfectly formed after the relaxation according to the GGA calculation. The relaxed geometry has the values of $a \approx b \neq c$ which implies that the relaxed structure is tetragonal with c/a ratio ≈ 0.988

Fig. 2 Calculated dispersion curves for ice (a) with no effective charges Z^* taken into account and (b) with Z^* taken into account. The curve on the left is the integrated phonon density of states. The frequencies ν_1 , ν_2 , are ν_3 are respectively bending, symmetric and anti-symmetric stretching analogous to the vibrational mode of an isolated water molecule [14]. Note that the vibrational phonon density of states is not complete as it requires summation over all points in the first Brillouin zone, nevertheless the calculated $G(\omega)$ for both with and without Z^* do not differ.

Fig. 3 Phonon dispersion in the transitional region showing the splitting of LO mode in the translational region. The dispersions are compared for the cases of both with and without the dipole interaction through the calculation of effective charges Z^* . The case with Z^* is marked by a^* . The experimental dispersion ([3] taken from [2]) is shown on the right

Fig. 4 Phonon dispersion in the librational, bending and stretching region showing the splitting of LO modes. The case with Z^* is marked by a^* as in Fig. 3

Table I: Adeagbo et. al

Dielectric constant in cartesian axis

(1.881163770	-0.000048586	-0.000019997)
(-0.000048586	1.881154759	0.000112163)
(-0.000019996	0.000112161	1.883382267)

Effective charges E-U in cartesian axis

Water molecule (1)	(hydrogen atom 1)			
(0.66721	0.37702	0.40166)
(0.40921	0.53464	0.38200)
(0.40785	0.36304	0.62434)
Water molecule (1)	(hydrogen atom 2)			
(0.66611	-0.37720	0.40208)
(-0.40909	0.53493	-0.38272)
(0.40784	-0.36353	0.62525)
Water molecule (2)	(hydrogen atom 1)			
(0.66619	0.37729	-0.40199)
(0.40909	0.53496	-0.38262)
(-0.40785	-0.36360	0.62507)
Water molecule (2)	(hydrogen atom 2)			
(0.66694	-0.37691	-0.40154)
(-0.40907	0.53471	0.38197)
(-0.40768	0.36296	0.62440)
Water molecule (3)	(hydrogen atom 1)			
(0.53461	0.40937	-0.38251)
(0.37708	0.66692	-0.40207)
(-0.36332	-0.40814	0.62483)
Water molecule (3)	(hydrogen atom 2)			
(0.53459	-0.40938	0.38266)
(-0.37714	0.66694	-0.40229)
(0.36338	-0.40822	0.62507)
Water molecule (4)	(hydrogen atom 1)			
(0.53516	-0.40898	-0.38225)
(-0.37710	0.66634	0.40159)
(-0.36333	0.40759	0.62478)
Water molecule (4)	(hydrogen atom 2)			
(0.53515	0.40892	0.38210)
(0.37715	0.66626	0.40141)
(0.36335	0.40747	0.62434)
Water molecule (5)	(hydrogen atom 1)			
(0.66666	-0.37682	-0.40144)
(-0.40902	0.53480	0.38199)
(-0.40761	0.36297	0.62446)

Water molecule (5)	(hydrogen atom 2)
(0.66648	0.37748 -0.40192)
(0.40929	0.53519 -0.38256)
(-0.40784	-0.36361 0.62469)
Water molecule (6)	(hydrogen atom 1)
(0.66694	0.37695 0.40158)
(0.40919	0.53476 0.38206)
(0.40781	0.36307 0.62443)
Water molecule (6)	(hydrogen atom 2)
(0.66639	-0.37738 0.40199)
(-0.40926	0.53512 -0.38263)
(0.40780	-0.36352 0.62484)
Water molecule (7)	(hydrogen atom 1)
(0.53456	0.40948 -0.38257)
(0.37720	0.66723 -0.40225)
(-0.36340	-0.40832 0.62487)
Water molecule (7)	(hydrogen atom 2)
(0.53464	-0.40928 0.38261)
(-0.37704	0.66666 -0.40213)
(0.36332	-0.40807 0.62503)
Water molecule (8)	(hydrogen atom 1)
(0.53514	0.40901 0.38225)
(0.37720	0.66637 0.40161)
(0.36345	0.40765 0.62469)
Water molecule (8)	(hydrogen atom 2)
(0.53515	-0.40887 -0.38209)
(-0.37703	0.66620 0.40138)
(-0.36322	0.40739 0.62441)
Water molecule (1)	(oxygen atom 1)
(-1.08499	-0.00011 -0.07462)
(0.00002	-0.96152 0.00068)
(-0.09759	0.00062 -1.07021)
Water molecule (2)	(oxygen atom 2)
(-1.08486	-0.00006 0.07446)
(-0.00023	-0.96140 0.00063)
(0.09737	0.00068 -1.07026)
Water molecule (3)	(oxygen atom 3)
(-0.96205	0.00002 -0.00017)
(-0.00008	-1.08534 0.07521)
(-0.00013	0.09795 -1.06997)
Water molecule (4)	(oxygen atom 4)
(-0.96115	0.00000 -0.00001)
(-0.00008	-1.08473 -0.07392)
(0.00006	-0.09639 -1.07014)
Water molecule (5)	(oxygen atom 5)

(-1.08488	-0.00031	0.07430)
(-0.00036	-0.96143	0.00038)
(0.09733	0.00058	-1.07024)
Water molecule (6)		(oxygen atom 6)		
(-1.08501	0.00014	-0.07445)
(0.00014	-0.96156	0.00039)
(-0.09755	0.00049	-1.07018)
Water molecule (7)		(oxygen atom 7)		
(-0.96206	-0.00013	-0.00004)
(-0.00004	-1.08536	0.07520)
(0.00010	0.09795	-1.06999)
Water molecule (8)		(oxygen atom 8)		
(-0.96113	0.00011	-0.00001)
(0.00005	-1.08471	-0.07392)
(-0.00004	-0.09639	-1.07012)

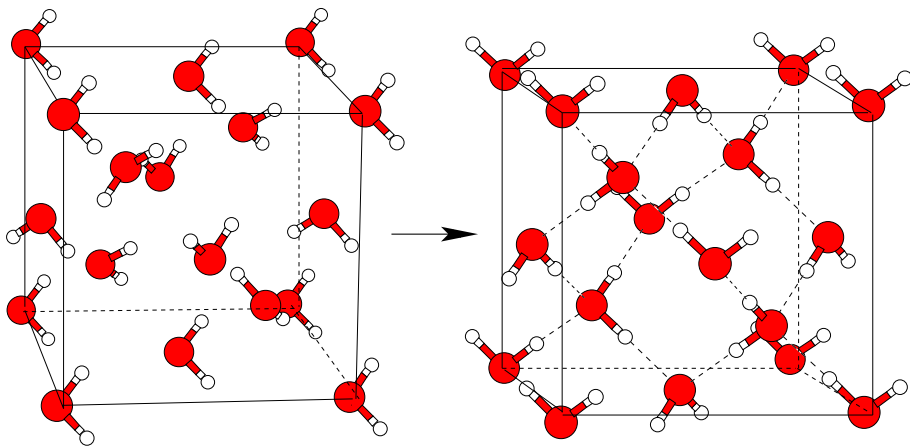


Figure 1: Adeagbo et al.

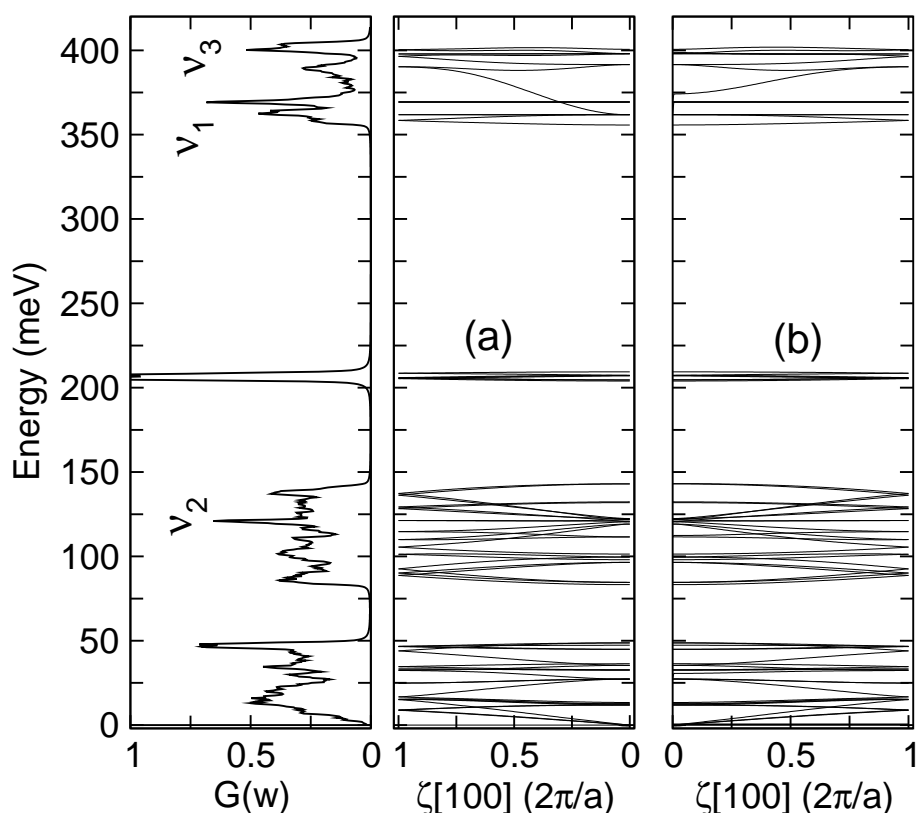


Figure 2: Adeagbo et al.

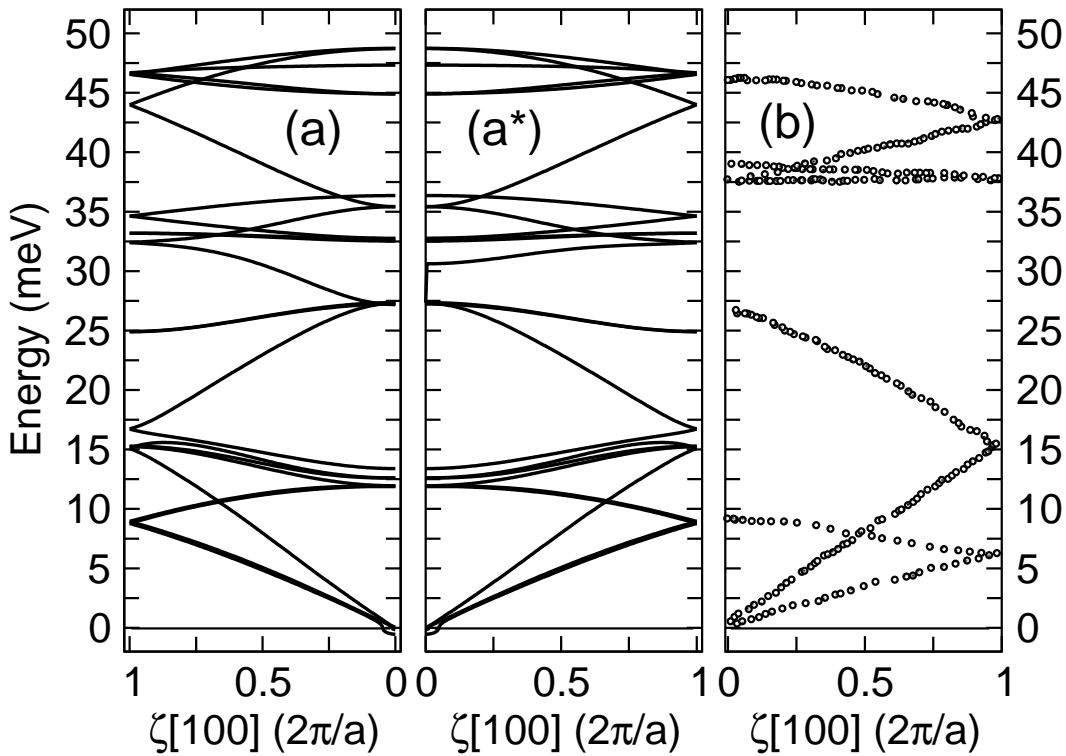


Figure 3: Adeagbo et al.

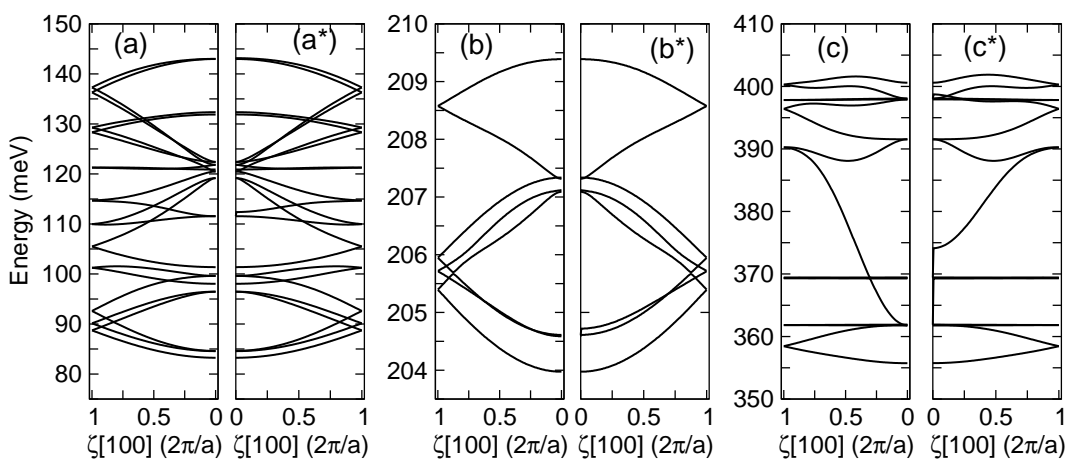


Figure 4: Adeagbo et al.